The Astronomical Journal, 123:1050–1055, 2002 February

THERMAL PROPERTIES OF CENTAURS ASBOLUS AND CHIRON

Yanga R. Fernández,[1] David C. Jewitt,[1] and Scott S. Sheppard
Institute for Astronomy, University of Hawaii at Manoa, 2680 Woodlawn Drive, Honolulu, HI 96822; yan@ifa.hawaii.edu, jewitt@ifa.hawaii.edu, sheppard@ifa.hawaii.edu
Received 2001 September 3; accepted 2001 October 29

ABSTRACT

We have measured the mid-infrared thermal continua from two Centaurs, inactive (8405) Asbolus and active 95P = (2060) Chiron, and have constrained their geometric albedos, p, and effective radii, R, with the standard thermal model for slow rotators. These are the first such measurements of Asbolus; we find $R = 33 \pm 2$ km and $p = 0.12 \pm 0.03$. This albedo is higher than all of those confidently known for active cometary nuclei. The thermal inertia is comparable to or lower than those of main-belt asteroids, the Moon, and Chiron; lower than those of the icy Galilean satellites; and much lower than those of near-Earth asteroids. For Chiron, we find $R = 74 \pm 4$ km and $p = 0.17 \pm 0.02$. While this albedo is consistent with the established value, previous radiometry by others implied a larger radius. This discrepancy may be partially due to a varying infrared dust coma, but all data sets have too low signal to be sure. Four Centaur albedos (out of about 30 objects) are now known. They show a diversity greater than that of the active comets, to which they are evolutionarily linked.

Key words: comets: individual (95P/Chiron) — minor planets, asteroids

1. INTRODUCTION

The so-called Centaur population consists of objects with perihelia beyond Jupiter but orbital semimajor axes smaller than Neptune's. Their orbits are unstable on timescales of about $10^{5.5}$ to $10^{6.5}$ yr (Dones, Levison, & Duncan 1996) as a result of perturbations by the giant planets and are in dynamical transition from the trans-Neptunian Kuiper belt to the inner solar system. Those Centaurs that are not thrown from the solar system or do not impact planets or the Sun are transferred into typical Jupiter-family comet-like orbits; thus, the Centaurs hold a direct evolutionary link between the cometary and trans-Neptunian populations. The colors of many Centaurs, extinct comet candidates, and active comets (Hartmann, Tholen, & Cruikshank 1987; Luu 1993) are consistent with this dynamical picture, and further physical and compositional studies will let us understand the physical evolution. Moreover, since the Centaurs are generally brighter than the trans-Neptunian objects (TNOs), they provide a proxy through which we can infer the ensemble properties of that more distant population.

The spectral diversity of the Centaurs and TNOs is well established (e.g., Luu & Jewitt 1996; Davies et al. 1998; Jewitt & Luu 1998; Barucci, Lazzarin, & Tozzi 1999), but the primary cause of this phenomenon is unknown. A secondary cause is probably the competition between reddening by cosmic-ray–induced surface chemistry and impacts exposing subsurface icy material (Jewitt & Luu 2001). Such a mechanism might also have observable effects on the albedo as a function of object size and color. Furthermore, cometary activity, for example, as shown by Chiron, may significantly influence the albedo as icy grains on ballistic trajectories dust the surface. Thus, sampling the Centaur and TNO albedos could provide clues to the physical nature of their surfaces.

In this paper, we describe the determination of the geometric albedos and sizes of two Centaurs, Chiron and Asbolus, using the radiometric method. We will place the Chiron data set in the context of earlier work by Lebofsky et al. (1984), Campins et al. (1994), Altenhoff & Stumpff (1995), and Groussin, Peschke, & Lamy (2000).

2. OBSERVATIONS AND REDUCTION

The observations span two wavelength regimes, mid-infrared (MIR) and visible. The MIR data were obtained with the Keck I Telescope using the "LWS" 256^2 pixel camera (Jones & Puetter 1993), and the visible-wavelength data were obtained with the University of Hawaii 2.2 m telescope using a Tektronix 2048^2 pixel CCD. Table 1 gives the observational circumstances of the two targets and the measured fluxes. The objects were unresolved at MIR wavelengths. No visible-wavelength data were obtained for (8405) Asbolus, so for our analysis we use results published by others.

The MIR data were obtained using chopping and nodding, both with throws of 4″. Nonsidereal guiding was used for each target. Flat fields were obtained by comparing staring images taken at both high and low air mass. The seeing was about 0.″3 FWHM at 12.5 μm and 0.″45 FWHM (diffraction limited) at 17.9 μm. Flux calibration was done by comparing count rates with the following known (12.5 and 17.9 μm) flux densities of standard stars: α Lyr, 26.4 and 12.9 Jy; σ Lib, 120.7 and 58.9 Jy; α CrB, 3.64 and 1.97 Jy; γ Aql, 54.2 and 27.5 Jy. These values are derived from the standard system in use at UKIRT (Chrysostomou 1998)[2] and the magnitudes given by Tokunaga (1984). We corrected for atmospheric extinction by comparing the stars' photometry over a range of air masses. As the filters we used are only 10% wide, the correction to monochromatic magnitudes was 0.01 mag or less and so was ignored.

The visible-wavelength image was obtained while guiding on a nearby star at a sidereal tracking rate in seeing that was

[1] Visiting Astronomer at W. M. Keck Observatory, which is jointly operated by the California Institute of Technology and the University of California.

[2] This information is available at http://www.jach.hawaii.edu/JACpublic/UKIRT/astronomy/conver.html.

TABLE 1
OBSERVING CIRCUMSTANCES

Date (UT)	Time (UT)	Exp. (s)	Air Mass	λ (μm)	r (AU)	Δ (AU)	α (deg)	Flux Density (mJy)
(2060) Chiron:								
2000 Jun 21.....	0931	324	1.25	12.5	10.109	9.139	1.79	14.4 ± 1.8
	1002	324	1.28	12.5	10.109	9.139	1.79	18.2 ± 2.7
2000 Jun 23.....	1042	324	1.39	12.5	10.113	9.153	1.98	14.3 ± 1.7
	1058	309	1.45	17.9	10.113	9.153	1.98	43.9 ± 15.9
	1114	309	1.52	17.9	10.113	9.153	1.98	56.4 ± 16.8
2000 Jul 1	0954	120	1.35	0.65	10.127	9.218	2.70	16.30 ± 0.01 mag[a]
(8405) Asbolus:								
2000 Jun 21.....	0854	324	1.91	12.5	7.867	6.988	3.94	17.0 ± 3.0
	0911	324	1.96	12.5	7.867	6.988	3.94	19.7 ± 2.7
2000 Jun 23.....	0840	324	1.90	12.5	7.862	6.998	4.13	15.2 ± 1.9
	0857	309	1.94	17.9	7.862	6.998	4.13	50.4 ± 15.7

NOTE.—"Exp." gives the on-source integration time. The wavelength of observation is λ. The heliocentric and geocentric distances are r and Δ, respectively. The phase angle is α.
[a] Object was not a point source. We used a circular synthetic aperture of radius 1.″1.

1″ FWHM. A flat field was constructed by combining dithered images of the blank twilight sky. Flux calibration and air-mass corrections were obtained by repeated measurements of the Landolt (1992) standard stars SA 107-457, 104-485, and 112-250. Chiron displayed a faint coma, as was expected, but the light was dominated by the nucleus. We used an aperture of radius 1.″1 to minimize the coma's contribution.

3. ANALYSIS

3.1. *Thermal Model*

The basic radiometric method to obtain an effective radius, R, and geometric albedo, p, is to solve two equations with these two unknowns, first done about 30 years ago (Allen 1970; Matson 1972; Morrison 1973) and described in detail by Lebofsky & Spencer (1989):

$$F_{\rm vis}(\lambda_{\rm vis}) = \frac{F_\odot(\lambda_{\rm vis})}{[r/(1\ {\rm AU})]^2}\pi R^2 p \frac{\Phi_{\rm vis}}{4\pi\Delta^2}\ , \tag{1a}$$

$$F_{\rm mir}(\lambda_{\rm mir}) = \epsilon\int B_\nu(T(pq,\theta,\phi),\lambda_{\rm mir})d\phi\, d(\cos\theta)R^2\frac{\eta\Phi_{\rm mir}}{4\pi\Delta^2}\ , \tag{1b}$$

where F is the measured flux density (in, e.g., W m^{-2} Hz^{-1}) of the object at wavelength λ in the visible ("vis") or mid-infrared ("mir"); $F_\odot$ is the flux density of the Sun at Earth as a function of wavelength; r and Δ are the object's heliocentric and geocentric distances, respectively; Φ is the (dimensionless) phase function in each regime; B_ν is the Planck function (in, e.g., W m^{-2} Hz^{-1} sr^{-1}); ϵ is the (dimensionless) infrared emissivity; η is a (dimensionless) factor to account for infrared beaming; and T is the temperature. The temperature itself is a function of the geometric albedo p, surface planetographic coordinates θ and ϕ, and the (dimensionless) phase integral q, which links the geometric and Bond albedos. For lack of detailed shape information—as is the case for our two objects—the modeled body is assumed to be spherical.

We employ the "standard thermal model" (STM) for slow rotators (Lebofsky et al. 1986) to derive the function T and evaluate equations (1a)–(1b). In the STM, the rotation is assumed to be so slow and/or the thermal inertia so small that every point on the surface is in instantaneous equilibrium with the impinging solar radiation. We will show below that the other extreme, a model assuming a fast rotator with a rotation axis perpendicular to the Sun-Earth-object plane, is inconsistent with the measured color temperatures.

The other parameters to the models are ϵ, η, $\Phi_{\rm mir}$, $\Phi_{\rm vis}$, and q. Emissivity is close to unity, and we will assume $\epsilon = 0.9$ here. The beaming parameter is known for only a few of the largest asteroids, but to facilitate comparison with other work, we adopt the standard value $\eta = 0.756$ (Lebofsky et al. 1986). For $\Phi_{\rm mir}$ we assume that the magnitude scales with the phase angle α: $-2.5\log\Phi_{\rm mir} = \beta\alpha$, where, based on earlier work (Matson 1972; Lebofsky et al. 1986), 0.005 mag deg$^{-1} \le \beta \le 0.017$ mag deg^{-1}. In the much better studied visible regime, we use the (H, G)-formalism (Lumme & Bowell 1981; Roemer, Candy, & Hers 1985) to obtain $\Phi_{\rm vis}$. The slope parameter G ranges between 0.0 and 0.7. The value of G determines q, but since that has a minor effect on the modeling, we adopt $q = 0.38$, the integral's value for $G = 0.15$. Note that our observations all occurred at small α (Table 1).

We should note that the values for R and p are valid in the context of the model used, but since the thermal model represents an extremum of thermal behavior, it is not a perfect descriptor. The error bars here and in many other published reports usually do not describe the systematic errors from the model itself. However, such errors are likely to be comparable to the quoted formal errors, so the values are still physically meaningful.

3.2. *Modeling Results for Asbolus*

We did not obtain our own visible-wavelength measurements of Asbolus, but photometry by Brown & Luu (1997) provides an excellent constraint. They measured a mean absolute magnitude[3] of $H = 8.43 \pm 0.05$ in the R band. Since our MIR measurements were taken at an unknown rotational phase, and the peak-to-valley amplitude is about 0.4 mag, we adopt a ± 0.2 mag uncertainty. With this visible-

[3] Absolute magnitude is the hypothetical apparent magnitude of an object when 1 AU from Earth, 1 AU from the Sun, and at zero phase angle.

wavelength information and our June 23 MIR photometry (see Table 1), the STM provides T and equations (1a)–(1b) yield Asbolus's effective radius R and geometric albedo p. Since there are not enough data points to perform the χ^2 statistical test, we have found instead the range of values for R and p such that the model passes within 2 σ of all data points. The ranges, means ($\bar{R}$ and $\bar{p}$), and standard deviations are

$$\bar{R} = 33 \pm 2 \text{ km}, \quad 29 \text{ km} \leq R \leq 38 \text{ km} ; \tag{2a}$$

$$\bar{p} = 0.12 \pm 0.03, \quad 0.06 \leq p \leq 0.20 . \tag{2b}$$

We note that the object was a few millijanskys brighter on June 21 compared with June 23; the time difference is 5.35 rotation periods (Brown & Luu 1997; Davies et al. 1998), and the magnitude difference is 0.20 ± 0.18. This is consistent with rotational modulation caused by a changing cross section, since in that case the MIR and visible amplitudes would be the same. However, we do not know the exact rotational phase of the MIR data, since the uncertainty in the magnitude difference is too large. (Otherwise we could find the position on a sine curve corresponding to that shift in rotation phase and change in brightness.) At worst, our data correspond to a minimum or maximum in brightness, but a 0.20 mag shift would affect R by only about 1% (since the object is dark) and p by 15% to 20%.

The STM predicts a (12.5 to 17.9 μm) color temperature of $T_c = 135$ K, while our photometry shows $T_c = 144 \pm 13$ K. By comparison, the fast-rotator model mentioned previously predicts $T_c = 100$ K, so that model is inapplicable. Since the spin period of Asbolus is not exceptionally slow—about 8.9 hr (Brown & Luu 1997; Davies et al. 1998)—the other contributing effect, the thermal inertia, must be low. A caveat is that the fast-rotator model degenerates into the slow-rotator model for a rotation axis pointing at the Sun, which could deceive us in interpreting the thermal inertia. However, the facts that (1) Asbolus has a large photometric amplitude (Brown & Luu 1997) and (2) Kern et al. (2000) have reported spectroscopic variation over the course of a rotation make a pole-on point of view unlikely. Note that the lack of rotational context prevents us from matching our albedo to the reported spectroscopic variation.

Given that the object is a slow rotator, we can calculate an upper limit to the thermal inertia. The dimensionless thermal parameter Θ, introduced by Spencer, Lebofsky, & Sykes (1989), is defined as

$$\Theta = \frac{\Gamma \sqrt{\omega}}{\epsilon \sigma T_{\rm SS}^3} , \tag{3}$$

where Γ is the thermal inertia, ω is the rotational frequency, σ is the Stefan-Boltzmann constant (in, e.g., W m^{-2} K^{-4}), and $T_{\rm SS}$ is the subsolar equilibrium temperature. This parameter is less than unity for a slow rotator (and zero for a body that is nonrotating or has no thermal inertia), and greater than unity for a fast rotator. Thermal inertia itself is defined as $\Gamma = (\kappa \rho c)^{1/2}$, where ρ is the object's bulk density (in, e.g., kg m^{-3}), c is the heat capacity (in, e.g., J kg^{-1} K^{-1}), and κ is the conductivity (in, e.g., W m^{-1} K^{-1}). Thus, Γ gives clues to the internal thermal behavior. At Asbolus's heliocentric distance (with $\epsilon = 0.9$, $p = 0.12$, and $q = 0.4$) $T_{\rm SS} = 142$ K, so $\Theta \leq 1$ requires that $\Gamma \leq 10.5$ J m^{-2} s$^{-1/2}$ K^{-1}. By comparison, in the same units, comet Halley's value for its active regions is 40 to 400 (Julian, Samarasinha, & Belton 2000) Ceres' value is about 10 (Spencer 1990); the Moon, 50 (Winter & Saari 1969); Europa, about 45 to 70 (Spencer et al. 1999), Ganymede, 70 (Spencer 1987); near-Earth asteroid Eros, 170 (Harris & Davies 1999); and near-Earth asteroid Phaethon, over 320 (Harris, Davies, & Green 1998). Asbolus's limit of 10.5 argues for a relatively porous and/or rough surface—perhaps a regolith, perhaps the aftermath of episodic cometary activity—inhibiting heat flow.

3.3. *Modeling Results for Chiron*

With our visible-wavelength and 12.5 μm photometry from Table 1, the STM provides T and equations (1a)–(1b) yield Chiron's effective radius R and geometric albedo p. Again, since there are not enough data points to permit the χ^2 statistical test, we have found instead the range of values for R and p such that the model passes within 2 σ of all data points. The ranges, means, and standard deviations are

$$\bar{R} = 74 \pm 4 \text{ km}, \quad 67 \text{ km} \leq R \leq 82 \text{ km} ; \tag{4a}$$

$$\bar{p} = 0.17 \pm 0.02, \quad 0.13 \leq p \leq 0.21 . \tag{4b}$$

We note that Chiron appeared slightly brighter on June 21 compared with June 23 (Table 1), but the magnitude difference, 0.14 ± 0.17, is consistent with the absence of a change. Since Chiron has a small rotational amplitude, 0.1 mag or less, this is expected and finding the rotational context is not as critical as for Asbolus.

The STM predicts a (12.5 to 17.9 μm) color temperature of $T_c = 120$ K. Our photometry shows $T_c = 155 \pm 20$ K, which is about 1.75 σ higher but clearly a better match than the fast-rotator model, which predicts $T_c = 88$ K. Since the spin period of Chiron is not exceptionally slow—about 5.9178 hr (Luu & Jewitt 1990; Marcialis & Buratti 1993)—the thermal inertia must be low. The same inertia caveat as for Asbolus may be applied here, but there is some evidence that we do not view the axis pole-on. The photometric variation due to rotation, which is less than 0.1 mag (Luu & Jewitt 1990), does not change with ecliptic longitude after accounting for damping by the coma (Marcialis & Buratti 1993).

Independently, Groussin et al. (2000) have used a "mixed model" thermal model of Chiron's surface, integrating the thermal properties of water ice and refractory grains, to constrain the thermal inertia from *Infrared Space Observatory* ISOPHOT mid- and far-infrared photometry (Peschke 1997). They obtain $\Gamma = 10$ J m^{-2} s$^{-1/2}$ K^{-1}, similar to Asbolus's limiting value from above.

Critical for the determination of the albedo is a robust measurement of the nucleus's visible-wavelength flux density without contamination from comatic light. As a check, we can compare our measured magnitude with the long-term photometric behavior of Chiron. In early 1985, Chiron appears to have been at one of its intrinsically faintest points (Marcialis & Buratti 1993), judging by the light curve over the last 30 years (Lazzaro et al. 1997; Bus et al. 2001). Marcialis & Buratti (1993) report a V-band absolute magnitude $H_V = 6.84$, assuming the slope parameter $G \approx 0.7$. The uncertainty in G is high and introduces several tenths of a magnitude of uncertainty to H_V, so here we shall instead refer magnitudes to the phase angle of their observations, $\alpha = \alpha_0 = 3\overset{\circ}{.}19$ on UT 1985 January 19. This is convenient

not only because we avoid having to worry about most of the opposition surge, but also because Chiron had a similar phase angle during our visible-wavelength observations. Thus, whereas $H_V = V - 5 \log r\Delta + 2.5 \log \Phi_{\rm vis}(\alpha)$, let us define

$$H_{V,\alpha_0} = V - 5\log r\Delta + 2.5\log \Phi_{\rm vis}(\alpha) - 2.5\log \Phi_{\rm vis}(\alpha_0)\,. \quad (5)$$

From the data published by Marcialis & Buratti (1993) for UT 1985 January 19, we calculate that $H_{V,\alpha_0} = 6.96 \pm 0.01$.

Now, regarding our photometry, the phase angle was $\alpha = 2\overset{\circ}{.}70$. If $0.0 \leq G \leq 0.7$, which is a range that covers nearly all of the asteroids for which slope parameters are known, then $2.5 \log \Phi_{\rm vis}(\alpha) - 2.5 \log \Phi_{\rm vis}(\alpha_0) = 0.03 \pm 0.01$ mag. Chiron has nearly solar colors (Hartmann et al. 1990), so $V-R = 0.37$, and substituting the data from Table 1 into equation (5) yields $H_{V,\alpha_0} = 6.85 \pm 0.03$. Thus, Chiron was only about 0.11 mag brighter than its faintest point in early 1985. Since the rotational phase was unknown, effectively the difference is 0.11 ± 0.05 mag, but the nucleus provided about 90% of the measured flux density during our observations.

4. DISCUSSION

4.1. *Albedo Context*

Figures 1 and 2 display our current understanding of albedos among the Centaurs and related bodies. The data were taken from this work and from many other published sources; the plotted error bars are those cited by the various authors.

In Figure 1, we plot albedo versus effective radius (*top*) and versus perihelion distance (*bottom*). We have only included objects with both reliable radii and albedos, and we have excluded Pluto, since its surface is strongly influenced by atmospheric effects. A trend with perihelion would suggest that the albedo is altered by thermal processing from insolation, but there is no apparent correlation in the plot. The addition of active and dormant comets in the 2 to 5 AU range would be useful. A trend with radius among the outer solar system objects might imply a connection between the albedo and effects that depend on cross section (such as the impact rate), and here, if we calculate the linear correlation coefficient, there is a correlation on the 3 σ level (as also noted by Jewitt, Aussel, & Evans 2001). However, this correlation is solely due to Charon, at $R = 625$ km and $p = 0.38$.

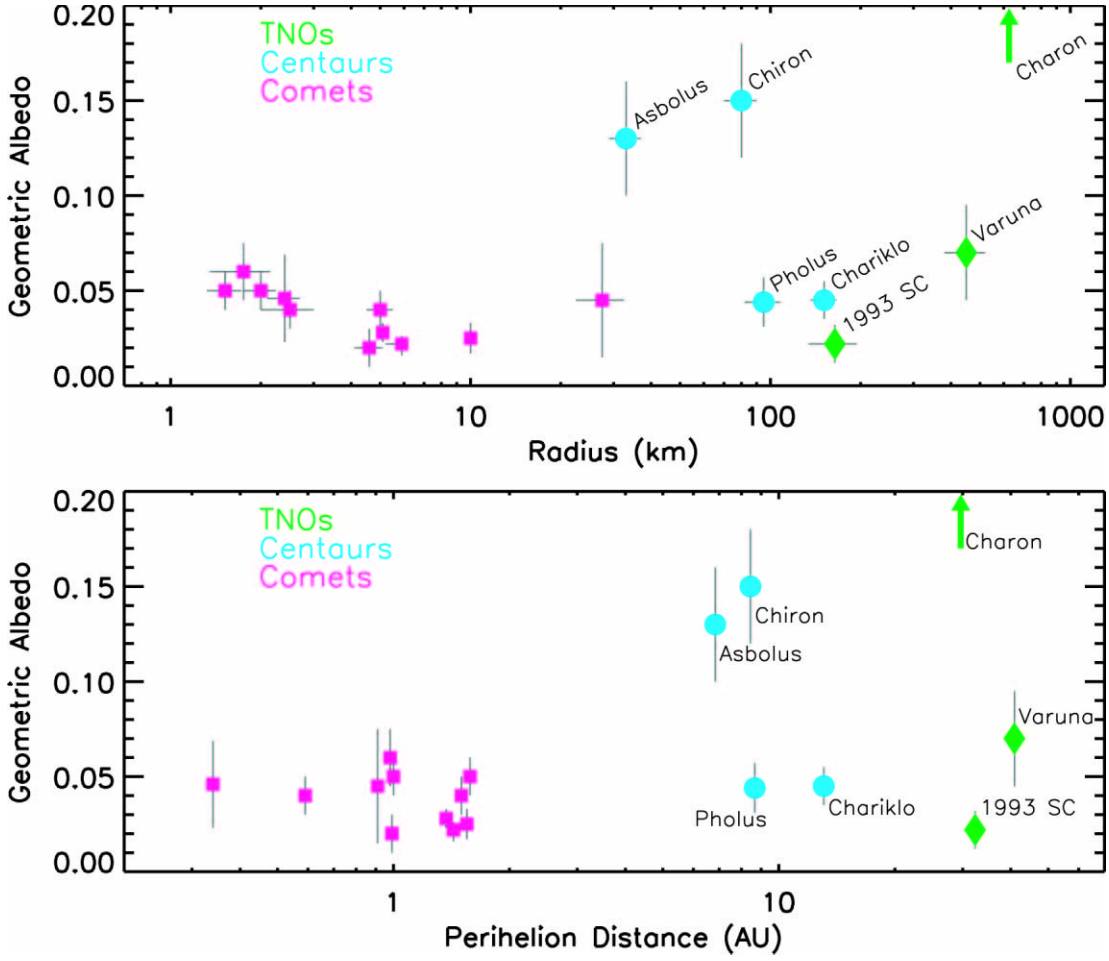

FIG. 1.—Plot of well-determined albedos vs. well-determined radii (*top*) and vs. perihelion distance (*bottom*). We have included only active comets (*squares*), Centaurs (*circles*), and trans-Neptunian objects (*diamonds*). For clarity of the other points, Charon (0.38 albedo) is off the top of each plot. Error bars are reported 1 σ. With four objects, the Centaurs already have a greater diversity in albedo than the known cometary nuclei. The plotted data were obtained from this work, A'Hearn et al. (1989), Campins, A'Hearn, & McFadden (1987), Campins et al. (1994, 1995), Davies et al. (1993), Fernández (1999), Fernández et al. (2002), Hanner et al. (1985), Jewitt et al. (2001), Jewitt & Kalas (1998), Jorda et al. (2000), Keller et al. (1986), Millis, A'Hearn, & Campins (1988), Sekanina (1988), and Thomas et al. (2000).

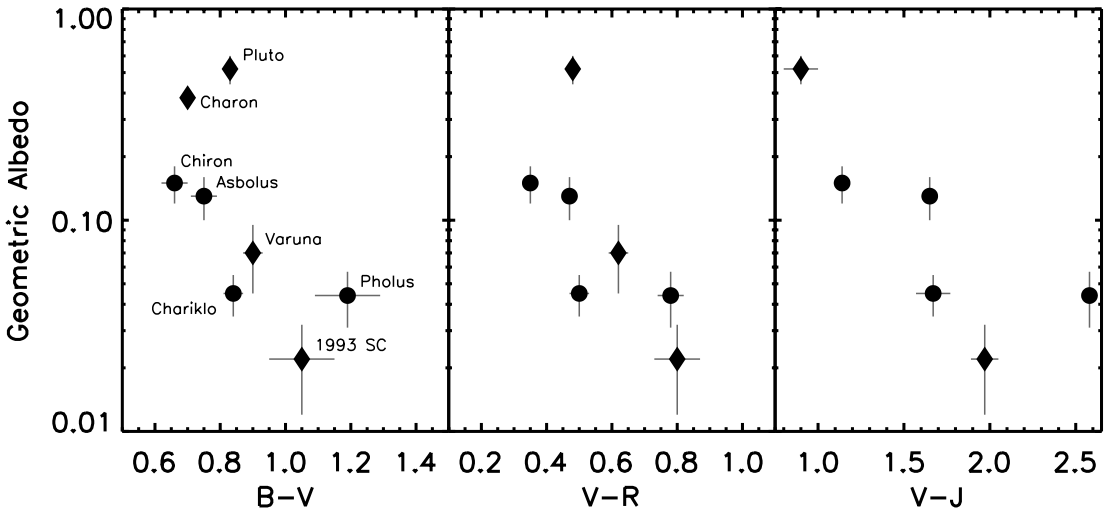

FIG. 2.—Plot of well-determined albedos and known $B-V$, $V-R$, and $V-J$ colors. Symbol shapes are the same as for Fig. 1. There is a general trend of redder objects being darker, although the sampling will have to be improved before there is high confidence in this conclusion, since many of the objects in the plot are atypical. The color data were obtained from Binzel (1988), Brown & Luu (1997), Davies et al. (1998), Hartmann et al. (1990), Jewitt & Luu (1998, 2001), Jewitt & Sheppard. (2002), Luu & Jewitt (1996), Romanishin et al. (1997), and Sykes et al. (2000). We have used the Pluto-Charon systemic color for $V-R$ and $V-J$.

The distribution of albedos itself however readily reveals that there is a greater diversity among the Centaurs than among the comets. Activity might yield a spuriously high albedo—since in that case one could overestimate the visible-wavelength flux—but for the inactive Asbolus that is inapplicable. It appears that during the dynamical cascade from the Kuiper belt, through the Centaur region, and into the inner solar system, an object does not necessarily preserve its albedo. Whether this is just a bias in our sampling of differently sized objects—since we have not yet seen many Centaur-sized, inner solar system, active comets—remains to be seen. However, the effect may provide a clue to the mechanisms of cometary activity, since the phenomenon occurring on Chiron does not appear to leave behind the same dark, mantled surface as we infer on the cometary nuclei. For example, an object that erupts in the Centaur region may be exposing pristine ice and/or dust the surface with icy grains. This scenario would suggest that Asbolus may still be sporadically active or only recently have entered a quiescent state.

Figure 2 compares albedo with $B-V$, $V-R$, and $V-J$ colors. Again the population is sparse, but we note a general trend of redder objects having a lower albedo. This would be consistent with the idea that chemistry activated by cosmic-ray irradiation affects surface darkening and reddening—if there were a mechanism to brighten the surface in the first place. For the Centaurs, cometary activity could be that mechanism. Impacts contribute to the effect as well, but since most impactors are too small to cause widespread resurfacing, and since other color data now are inconsistent with the predicted manifestations, this cannot be the dominant cause (Jewitt & Luu 2001). The full explanation of the color diversity remains unknown, but in any case, populating Figure 2 with the albedos of more ordinary objects would be wise.

4.2. *Earlier Chiron Radiometry*

Table 2 gives a list of published radiometric estimates of Chiron's radius (with 1 σ uncertainties) and color temperature as a function of time and heliocentric distance. The average radius (weighted by the variances) is 82 km; on the 2 σ level all points are consistent. Some of the variation on the positive side would normally be attributed to contamination from the infrared dust coma, but this would not mimic the long-term trend in activity seen at visible wavelengths (Lazzaro et al. 1997). Moreover, a high color temperature is difficult to explain. Grains much smaller than the wavelength of peak Planck emission will appear to be hotter than expected, but if that were the case with Chiron, one would also expect the comet to be intrinsically brighter (and hence yield a larger effective radius), opposite to what is observed. A further constraint is the occultation result of Bus et al. (1996), where the assumed-spherical Chiron needs to have $R \geq 90$ km. Since rotational light curves imply that Chiron is indeed only about 10% aspherical (Bus et al. 1989), this would imply a minimum effective radius of about 85 km.

TABLE 2
CHIRON RADIOMETRIC RADII

UT Day	r (AU)	R (km)	T_c (K)	T_e (K)	Ref.	Note
1983 Jan 9/10	15.8	77^{+15}_{-19}	...	...	1	a
1991 Nov 18/19 ...	10.0	74 ± 11	143 ± 19	122	2	b
1993 Nov 22	8.9	96 ± 7	122 ± 10	129	2	c
1994 Mar 31	8.8	93 ± 5	136 ± 12	129	2	c
1994 Apr 27.....	8.8	84 ± 10	...	...	3	a
1996 Jun 8–15.....	8.5	80^{+3}_{-10}	115 ± 7	127	4	d
2000 Jun 21/23	10.1	74 ± 4	155 ± 20	121	5	b

NOTE.—Heliocentric distance is r, effective radius is R, measured color temperature is T_c, and the expected color temperature from the thermal model is T_e. Perihelion occurred on 1996 February 15.

[a] Only one wavelength was measured, so color not applicable.

[b] Reported R is from just one of the wavelengths.

[c] Listed R is weighted average of the reported results.

[d] Used 25 and 60 μm data to calculate T_c and T_e.

REFERENCES.—(1) Lebofsky et al. 1984; (2) Campins et al. 1994; (3) Altenhoff & Stumpff 1995; (4) Groussin et al. 2000; (5) this work.

The reconciliation of the radiometry in Table 2 (and the occultation data) may involve more detailed thermal modeling, as Groussin et al. (2000) have done, but further observations are certainly necessary, since none of the thermal measurements in the past 20 years have high signal-to-noise ratio. Thus it is possible that photometric uncertainty is corrupting our interpretation.

Lastly, we note that the albedo in equation (4b) is consistent with previous values (Campins et al. 1994). Since our visible photometry is about 0.1 mag brighter than the faintest intrinsic measurements, as discussed in § 3.3, such a correction would reduce our albedo by 0.015. Groussin et al. (2001) report an albedo of 0.12 ± 0.02 using $H_V = 6.95 \pm 0.2$, which would make Chiron about 0.3 mag intrinsically fainter than observed by Marcialis & Buratti (1993) in 1985. A correction of that size would further reduce our albedo by 0.037. Thus, all variation among reported albedos can be explained by the use of the different absolute magnitudes.

5. SUMMARY

1. We have radiometrically determined the effective radii R and geometric albedos p of Centaurs Asbolus and Chiron:

$$29 \text{ km} \leq R \leq 38 \text{ km}, \quad 0.06 \leq p \leq 0.20 \quad \text{for Asbolus;}$$
$$67 \text{ km} \leq R \leq 82 \text{ km}, \quad 0.13 \leq p \leq 0.21 \quad \text{for Chiron.}$$

The ranges effectively cover 2σ.

2. Under the STM formalism (Lebofsky et al. 1986; Spencer et al. 1989), we calculate an upper limit to Asbolus's thermal inertia of $\Gamma \leq 10.5$ J m^{-2} s$^{-1/2}$ K^{-1}. This value is comparable to those of main-belt asteroids, smaller than those of icy Galilean satellites, and an order of magnitude smaller than the few values known for near-Earth asteroids. Groussin et al. (2000) find a comparable value for the Γ of Chiron. Presumably the surfaces of Chiron and Asbolus are relatively porous and/or rough enough to inhibit heat flow.

3. Chiron's albedo is consistent with earlier measurements by others, taking into account the varying absolute magnitude, but others have noted a larger radius (at the 2σ level). Whether this is due to a varying infrared coma or simply the low signal-to-noise ratio of all extant radiometric data remains to be seen.

4. Of the four Centaur albedos now known, two are comet-like and two are 2 to 3 times higher. During the dynamical cascade of objects from the Kuiper belt and through the Centaur region into the inner solar system, the albedo is apparently not always preserved, although a more robust demonstration would require a comparison of similarly sized objects. Nevertheless, there is a greater diversity among the albedos of the Centaurs than of the cometary nuclei.

We thank Jane Luu for helpful comments on the manuscript. We gratefully acknowledge the help of Keck staff members Joel Aycock, Meg Whittle, Wayne Wack, and Greg Wirth, and 2.2 m staff member John Dvorak. We also acknowledge the JPL Solar System Dynamics Group for their Horizons on-line ephemeris generation program. This work was supported by grants to D. C. J. from NSF.

REFERENCES

A'Hearn, M. F., Campins, H., Schleicher, D. G., & Millis, R. L. 1989, ApJ, 347, 1155
Allen, D. A. 1970, Nature, 227, 158
Altenhoff, W. J., & Stumpff, P. 1995, A&A, 293, L41
Barucci, M. A., Lazzarin, M., & Tozzi, G. P. 1999, AJ, 117, 1929
Binzel, R. P. 1988, Science, 241, 1070
Brown, W. R., & Luu, J. X. 1997, Icarus, 126, 218
Bus, S. J., A'Hearn, M. F., Bowell, E., & Stern, S. A. 2001, Icarus, 150, 94
Bus, S. J., Bowell, E., Harris, A. W., & Hewitt, A. V. 1989, Icarus, 77, 223
Bus, S. J., et al. 1996, Icarus, 123, 478
Campins, H., A'Hearn, M. F., & McFadden, L.-A. 1987, ApJ, 316, 847
Campins, H., Osip, D. J., Rieke, G. H., & Rieke, M. J. 1995, Planet. Space Sci., 43, 733
Campins, H., Telesco, C. M., Osip, D. J., Rieke, G. H., Rieke, M. J., & Schulz, B. 1994, AJ, 108, 2318
Chrysostomou, A. 1998, Conversion of Magnitudes to Janskys and F-Lambda (Hilo: Joint Astron. Cent.)
Davies, J., Spencer, J., Sykes, M., Tholen, D., & Green, S. 1993, IAU Circ. 5698
Davies, J. K., McBride, N., Ellison, S. L., Green, S. F., & Ballantyne, D. R. 1998, Icarus, 134, 213
Dones, L., Levison, H. F., & Duncan, M. 1996, in ASP Conf. Ser. 107, Completing the Inventory of the Solar System, ed. T. W. Rettig & J. M. Hahn (San Francisco: ASP), 233
Fernández, Y. R. 1999, Ph.D. thesis, Univ. Maryland
Fernández, Y. R., Meech, K. J., Lisse, C. M., A'Hearn, M. F., Pittichová, J., & Belton, M. J. S. 2002, Icarus, submitted
Groussin, O., Peschke, S., & Lamy P. L. 2000, BAAS, 32, 1031
Hanner, M. S., Aitken, D. K., Knacke, R., McCorkle, S., Roche, P. F., & Tokunaga, A. T. 1985, Icarus, 62, 97
Harris, A. W., & Davies, J. K. 1999, Icarus, 142, 464
Harris, A. W., Davies, J. K., & Green, S. F. 1998, Icarus, 135, 441
Hartmann, W. K., Tholen, D. J., & Cruikshank, D. P. 1987, Icarus, 69, 33
Hartmann, W. K., Tholen, D. J., Meech, K. J., & Cruikshank, D. P. 1990, Icarus, 83, 1
Jewitt, D., Aussel, H., & Evans, A. 2001, Nature, 411, 446
Jewitt, D., & Kalas, P. 1998, ApJ, 499, L103
Jewitt, D., & Luu, J. 1998, AJ, 115, 1667
Jewitt, D. C., & Luu, J. X. 2001, AJ, 122, 2099
Jewitt, D. C., & Sheppard, S. S. 2002, AJ, in press
Jones, B., & Puetter, R. C. 1993, Proc. SPIE, 1946, 610
Jorda, L., Lamy, P., Groussin, O., Toth, I., A'Hearn, M. F., & Peschke, S. 2000, in *ISO* beyond Point Sources, ed. R. J. Laureijs, K. Leech, & M. F. Kessler (ESA SP-455) (Noordwijk: ESA), 61
Julian, W. H., Samarasinha, N. H., & Belton, M. J. S. 2000, Icarus, 144, 160
Keller, H. U., et al. 1986, Nature, 321, 320
Kern, S. D., McCarthy, D. W., Buie, M. W., Brown, R. H., Campins, H., & Rieke, M. 2000, ApJ, 542, L155
Landolt, A. U. 1992, AJ, 104, 340
Lazzaro, D., et al. 1997, Planet. Space Sci., 45, 1607
Lebofsky, L. A., & Spencer, J. R. 1989, in Asteroids II, R. P. Binzel, T. Gehrels, & M. S. Matthews (Tucson: Univ. Arizona Press), 128
Lebofsky, L. A., et al. 1986, Icarus, 68, 239
Lebofsky, L. A., Tholen, D. J., Rieke, G. H., & Lebofsky, M. J. 1984, Icarus, 60, 532
Lumme, K., & Bowell, E. 1981, AJ, 86, 1705
Luu, J., & Jewitt, D. 1996, AJ, 112, 2310
Luu, J. X. 1993, Icarus, 104, 138
Luu, J. X., & Jewitt, D. C. 1990, AJ, 100, 913
Marcialis, R. L., & Buratti, B. J. 1993, Icarus, 104, 234
Matson, D. L. 1972, Ph.D. thesis, Caltech
Millis, R. L., A'Hearn, M. F., & Campins, H. 1988, ApJ, 324, 1194
Morrison, D. 1973, Icarus, 19, 1
Peschke, S. B. 1997, Ph.D. thesis, Univ. Heidelberg
Roemer, E., Candy, M. P., & Hers, J. 1985, Trans. IAU, 19B, 177
Romanishin, W., Tegler, S. C., Levine, J., & Butler, N. 1997, AJ, 113, 1893
Sekanina, Z. 1988, AJ, 95, 1876
Spencer, J. R. 1987, Ph.D. thesis, Univ. Arizona
———. 1990, Icarus, 83, 27
Spencer, J. R., Lebofsky, L. A., & Sykes, M. V. 1989, Icarus, 78, 337
Spencer, J. R., Tamppari, L. K., Martin, T. Z., & Travis, L. D. 1999, Science, 284, 1514
Sykes, M., Cutri, R., Fowler, J., Tholen, D., & Skrutskie, M. 2000, IAU Circ. 7518
Thomas, N., et al. 2000, ApJ, 534, 446
Tokunaga, A. 1984, AJ, 89, 172
Winter, D. F., & Saari, J. M. 1969, ApJ, 156, 1135